GA–A22577

AN ELM-RESILIENT RF ARC DETECTION SYSTEM FOR DIII–D BASED ON ELECTROMAGNETIC AND SOUND EMISSIONS FROM THE ARC

by

D.A. PHELPS

APRIL 1997

GA–A22577

AN ELM-RESILIENT RF ARC DETECTION SYSTEM FOR DIII–D BASED ON ELECTROMAGNETIC AND SOUND EMISSIONS FROM THE ARC

by

D.A. PHELPS

This is a preprint of a paper presented at the 12th Topical Conference on Radio Frequency Power in Plasmas, April 1–3, 1997, Savannah, Georgia, and to be printed in the *Proceedings.*

Work supported by
U.S. Department of Energy Contract
DE-AC03-89ER51114

GENERAL ATOMICS PROJECT 3466
APRIL 1997

An ELM-Resilient RF Arc Detection System for DIII–D Based on Electromagnetic and Sound Emissions from the Arc

D.A. Phelps

General Atomics, San Diego, California 92186

Abstract. Two detection methods based solely on sound and electromagnetic emissions from the arc are presented. Detection of arc induced sound signals 40 to 50 dB above background noise are observed. Detection of arc induced low radio frequency (HF) electromagnetic noise levels 20 to 60 dB above background are observed. The arc noise is randomly strongest on side A and/or B of the DIII–D rf system. The sum of these sensors correlates with tripping due to an increase in the rf reflection coefficient. The sensors are resilient to ELMs and other plasma noise.

Present day Fast Wave Ion Cyclotron Range of Frequency (ICRF) transmitter systems are protected for load mismatch by systems that cannot discern an arc from an ELM. To maximize the rf power during ELMing H–mode using present antenna systems on DIII–D, a load mismatch system needs to be developed that reliably identifies an arc in the presence of ELMs. We are studying two detection methods based solely on sound and low radio frequency (HF) emissions from the arc. HF arc noise detection was first tested on C–Mod [1] and later on ASDEX Upgrade [2,3] and DIII–D [4].

The test bed for these concepts is the 285° antenna and transmission line system shown in Fig. 1. Each of the four elements is connected by a vacuum and pressurized transmission line that forms two standing wave resonant loops. Power from a transmitter is split by a 3 dB hybrid and then tuned to match sides A and B.

The proposed sound detectors are denoted by the symbols S1 through S12. Each detector is an electrostatically shielded piezoelectric ceramic sensor that is mounted flush to the metal outer conductor of the rf transmission line. The sound induced voltage signal is in the audio frequency. A signal processing system detects the envelope of the transient voltage and sends this to a digitizer for recording by the DIII–D computer system.

An example of the detected noise during an arc is shown in Fig. 2. Note that the detected forward power trips during the middle of the pulse and drops to zero

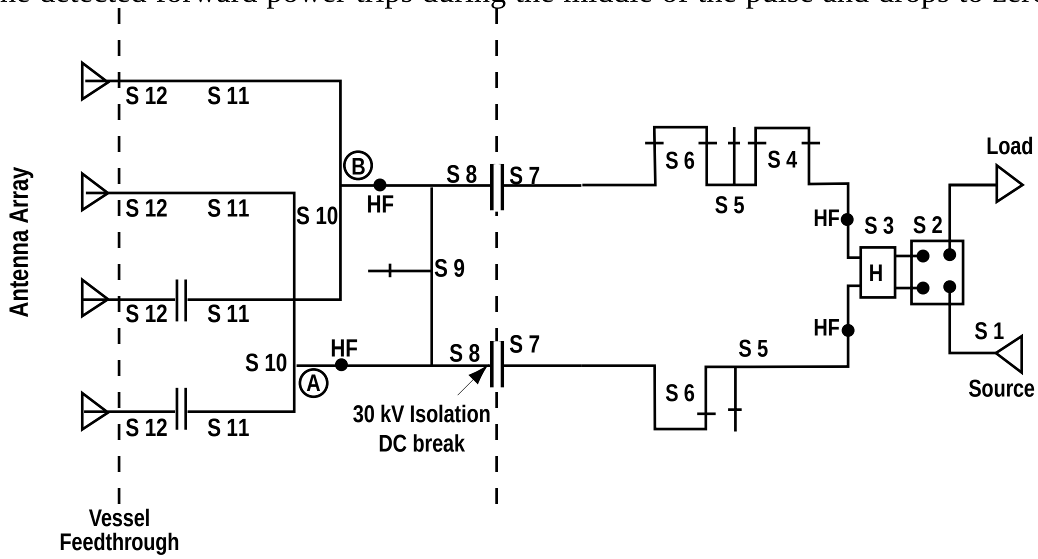

FIGURE 1. Layout of sound and rf detectors.

for a period that is required to clear the arc plasma in vacuum. At the same time a strong sound noise is detected by the S9 sensor in Fig. 1. In contrast, arc sound at sensors S10 are not detectable (sensors S8 have not been installed). This pinpoints the location of the arc near the rf decoupler stub.

The sound waves propagate more efficiently along the associated coaxial runs than through the air, but sounds are dispersive and hence a clear rising front edge due to the arc is not detected. This means a closer spacing between sensors is more required to pinpoint the arc using the peak of the detected noise envelope. Aiding this interpretation are the number of flanges through out the system that attenuate the sound noise. In addition, sensors on both sides of the dc breaks are needed because sound is muffled by the breaks.

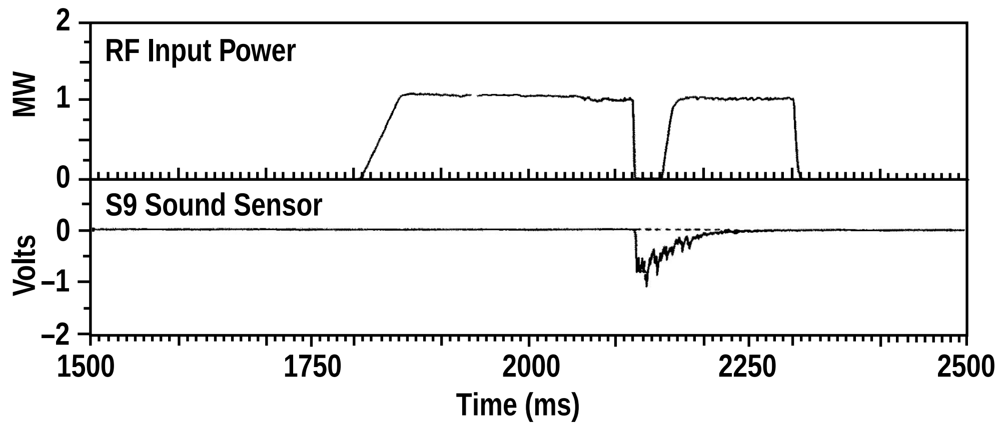

FIGURE 2. Sound emission from an arc.

The proposed HF arc detectors are denoted by the LF symbols in Fig. 1. Two voltage probes within the standing wave resonant line sense the rf noise at a voltage minimum for 60 MHz operation. These probes are yet to be implemented. The three detectors around the hybrid splitter use reflected power directional couplers (to minimize interference from the high power rf at 60 MHz). The high power rf is further reduced about 90 dB by passage through an 8–12 MHz filter. This filter suppresses lower frequency noise due to power supply switching transients and other operating system noise. The filter also suppresses undesirable noise emanating from the plasma, such as 20+ MHz noise during locked modes, large sawteeth, and bursts of radiation at the deuterium cyclotron frequency in the plasma edge [4]. The filter overlaps the spectrum of arc noise as shown in Fig. 3. The filtered output signal is detected using an HP 423B crystal, passed through a peak detector with a fast (l300 ns) risetime and a slow (1–10 ms) decay time. The peak signal is sent to the digitizer and recorded by the computer system.

Examples of arcs during vacuum conditioning and plasma operation are shown in Fig. 4. The signal peaks are typically 20 to 40 dB above the background noise. The signals in Fig. 4(a) run together because the peak detector decay time is optimized for a nominal 1 kHz sampling rate and many arcs occur close together during the vacuum conditioning. Note that arcs occur at the same and at different times on side A and B. This suggests that the rf noise is randomly occurring as expected during arcing. The smaller signals appearing between the transmitter and the hybrid are due to less amplification and to the difficulty of passing rf noise through the hybrid.

Note in Fig. 4(b) that the standard VSWR fault detector trips six times due to arcing. All arcs are detected by the combination of HF noise from sides A and B. This includes the vacuum arc that released nickel into the plasma. The ELM sensor in Fig. 4 indicates many ELM spikes. The rf arc noise is clearly independent of ELMs.

In conclusion, two detection methods based solely on sound and electromagnetic emissions from the arc have been presented. Clear evidence has been presented that sound noise can pinpoint rf arcs in the pressurized gas insulated coax

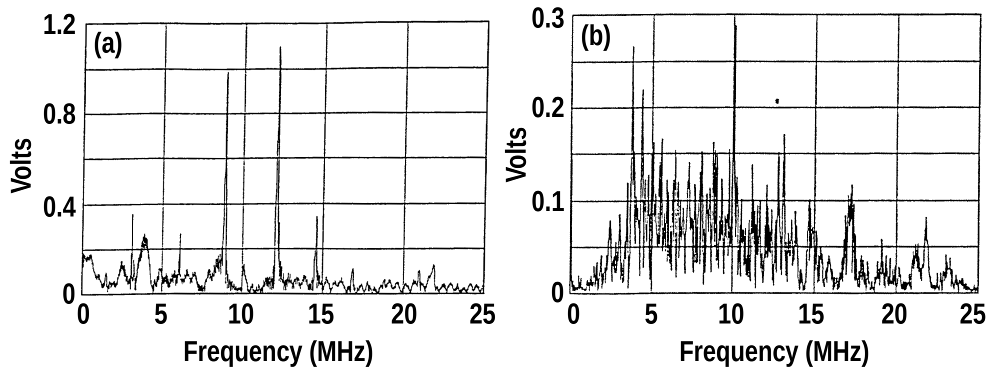

FIGURE 3. (a) Vacuum and (b) pressurized gas arcs observed on ASDEX Upgrade.

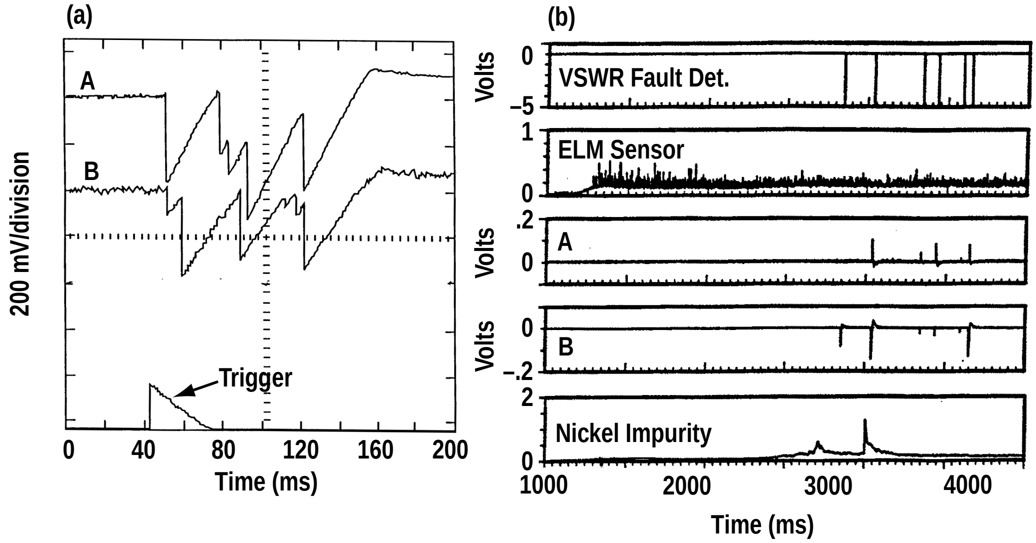

FIGURE 4. HF arcs detected during (a) vacuum conditioning and (b) plasma operation.

by displaying the strongest signal at the sensor closest to the arc. Furthermore, clear evidence that arcs during vacuum conditioning and plasma operation can be observed by an HF detector that does not respond to ELMs. Future arc sound and HF noise experiments are planned using additional sensors to remove present apparent blind spots in the 0°, 180°, and 285° antenna systems. The goal is 100% detection of arcs and no spurious signals due to power supply switching, high power rf signal interference, noise emanating from the plasma, or crosstalk between antenna systems.

This is a report of work sponsored by U.S. Department of Energy Contract DE-AC03-89ER51114.

REFERENCES

1. M. Fridberg *et al.*, ‘‘Upgrading the 80 MHz Transmitter on C–MOD, in *Proc. 15th Symp. Fusion Engineering*, Vol. 2, 1081 (1993).
2. F. Braun, ‘‘An Arc Detection System for ICRH,’’ to be published in *Proc. 19th Symp. Fusion Technol.*, Lisbon (1996).
3. F. Wesner *et al.*, ‘‘Status of ASDEX Upgrade,’’ to be published in *Proc. 12th Conf. on RF Power in Plasmas*, Savannah (1997).
4. J. H. Rogers *et al.*, ‘‘RF Arc Detection Using Harmonic Signals,’’ in *Proc. 16th Symp. Fusion Engineering*, Urbana (1995) Vol. 2, p. 522.